Validation of Photovoltaic Spectral Effects Derived From Satellite-Based Solar Irradiance Products

Sophie Pelland and Christian A. Gueymard

***Abstract*—The Satellite Application Facility on Climate Monitoring (CM-SAF) Spectral Resolved Irradiance (SRI) and National Renewable Energy Laboratory National Solar Radiation Database Spectral on Demand (NSRDB-S) satellite-based spectral irradiance products are tested here against benchmark data and models at seven ground stations: one in Spain for CM-SAF SRI and six in North America for NSRDB-S. Benchmarks include WISER spectroradiometers, spectra modeled from SolarSIM-G measurements and the SMARTS radiative code with two alternate input sources: AErosol RObotic NETwork (AERONET) and the Modern-Era Retrospective analysis for Research and Applications, Version 2 (MERRA-2) reanalysis. The satellite products are tested in terms of their ability to estimate photovoltaic (PV) spectral effects for six PV module technologies. The spectra are also compared directly under clear-sky conditions. Both CM-SAF SRI and NSRDB-S outperform the simple benchmark of neglecting spectral effects in terms of predicting instantaneous spectral mismatch factors, but only CM-SAF SRI generally does better at predicting long-term spectral derate factors. The clear-sky results reveal systematic differences between NSRDB-S and benchmark spectra, likely due to the NSRDB-S treatment of aerosols. Meanwhile, the mean SMARTS spectra with AERONET and MERRA-2 inputs are in good agreement, showing promise for the use of MERRA-2 as input to clear-sky models.**

***Index Terms*—Irradiance, mismatch, photovoltaic, satellite, solar, spectral.**

I. INTRODUCTION

PHOTOVOLTAIC (PV) modules are generally rated at Standard Test Conditions (STC), which include the AM1.5 reference spectral distribution of solar irradiance [1]. Deviations from this distribution under real operating conditions can lead to energy gains or losses on an annual basis of up to roughly 3% for crystalline silicon and 10% for amorphous silicon [2]. Ideally, spectral effects would be derived using PV module spectral responsivity and data from an on-site spectroradiometer, but this is usually not feasible since such ideal circumstance is extremely rare.

Instead, current photovoltaic modeling tools either ignore spectral effects altogether or approximate spectral effects using atmospheric variables that influence the spectral distribution of irradiance, such as clear-sky index, air mass, or integrated water vapor (see, e.g., [3]). While such models are easy to integrate into modeling tools and usually rely on commonly available data, they need to be trained with spectral responsivity data from specific PV modules. This means that the models need to be re-trained whenever the spectral responsivity of a PV module of interest differs significantly from those included in the model. Moreover, such models are usually empirical, in which case they must be trained on the limited number of available spectral irradiance data sets. Whereas a recent cross-validation analysis suggests that empirical models have skill in generalizing to new locations [3], the extent of this generalizability remains an open question.

In parallel, some satellite-based spectral irradiance products have become available in recent years [4, 5, 6], offering a promising alternative with broad geographic coverage. Unlike their broadband counterparts, however, there has been limited validation of these spectral products to date. The present study continues this validation effort by comparing two satellite-based spectral irradiance products to benchmark data and models at seven locations, with an emphasis on the skill of the satellite products at modeling PV spectral effects.

II. SATELLITE-BASED SPECTRAL IRRADIANCE PRODUCTS

So far, only two operational satellite-based spectral irradiance products appear to be available in the public domain: (i) the National Renewable Energy Laboratory (NREL) National Solar Radiation Database (NSRDB) Spectral On-Demand (NSRDB-S) service, and (ii) the Satellite Application Facility on Climate Monitoring (CM-SAF) Spectral Resolved Irradiance (SRI) data set. NSRDB-S covers parts of the Americas, whereas CM-SAF SRI covers parts of Europe, Africa, the Middle East, and South America. Both products are tested here.

The NSRDB-S service runs the Fast All-sky Radiation Model for Solar applications with Narrowband Irradiances on Tilted surfaces (FARMS-NIT) model [5, 6] on NREL's servers in real time. Atmospheric properties are derived using data from the Modern-Era Retrospective analysis for Research and Applications, Version 2 (MERRA-2) reanalysis [7], and parameterized based on some quantities extracted from version 2.9.5 of the Simple Model of the Atmospheric Radiative Transfer of Sunshine (SMARTS) [8]. Spectral data are currently available from 1998 to 2019 at an hourly time step, for any fixed-tilt PV array orientation and for one-axis trackers. They include 2002 wavebands ranging from 280 to 4000 nm.

Some FARMS-NIT spectra have been benchmarked against those of other radiative transfer models and against spectroradiometer data in Golden, Colorado, USA, under clear-sky conditions [5, 6]. The latter, location-specific comparison used model inputs from ground observations rather than MERRA-2, hence does not constitute a complete test of the NSRDB-S product per se.

The CM-SAF SRI spectral product is based on the SPECMAGIC model, with atmospheric inputs derived from

monthly mean and climatological data [4]. CM-SAF SRI spectral data are made available to users on a monthly mean basis, from 1983 to 2017, for 32 wavebands from 240–4606 nm [9]. The SPECMAGIC spectral irradiances have been tested against spectroradiometer data at two European locations, with results indicating uncertainty comparable to that of spectroradiometers themselves, except in the UV and near infrared (≥1200 nm) [10].

III. Benchmark Data

Appropriate measurements have been obtained for the seven ground stations shown in Fig. 1 (with latitudes ranging from 37.09 to 53.34°), for different time periods of at least one year in 2014, 2018, and 2019, and at time steps of 1–5 minutes, as described in [3]. Each of these stations monitors the broadband global horizontal irradiance (GHI), direct normal irradiance (DNI), and diffuse horizontal irradiance (DIF), along with other meteorological variables.

Stations in Golden and Almería, Spain, are equipped with EKO WISER I spectroradiometers that cover the 290–1650-nm (Golden) and 300–1700-nm (Almería) spectral ranges. In what follows, only measurements and model estimates of spectral *global horizontal* irradiance are considered. At Almería, spectral modeling was used by Deutsches Zentrum für Luft- und Raumfahrt (DLR) to extend the data to the 280–4000-nm range [11]. Quality control of data is described in [3], and additional DLR-conducted quality control at Almería is detailed in [11].
The remaining five stations are located across Canada in Varennes, Egbert, Charlottetown, Devon, and Ottawa. They include Spectrafy SolarSIM-G spectral irradiance sensors, which measure irradiance in nine narrow wavelength bands, and reconstitute the 280–4000-nm spectrum through proprietary software. In addition, the Egbert, Almería, and Golden locations include an AErosol RObotic NETwork (AERONET) station for at least a part of the period of interest. AERONET is a global network of stations [12] that are equipped with multiwavelength sunphotometers to observe the incident spectrum at typically 8 wavelengths in the 340–1640-nm range. After various quality-control steps (most importantly to remove periods when the sun disc is occluded by clouds), some key optical properties of aerosols and water vapor are derived using a sophisticated retrieval algorithm [13].

Spectroradiometric measurements at Golden and Almería are used here directly to test the satellite-based spectral global irradiance products. In parallel, and as described below, the SolarSIM-G, AERONET, and MERRA-2 data are also used as inputs to radiative transfer models to produce modeled spectra to serve as additional benchmarks.

Fig. 1. Location of the seven ground stations (©Google Earth Pro, 2022).

IV. Benchmark Models

Four benchmark models are used to further assess the performance of the NSRDB-S and CM-SAF SRI products: (i) ignoring all spectral effects; (ii) Spectrafy modeled spectra; and SMARTS modeled spectra with either (iii) AERONET or (iv) MERRA-2 inputs. For all these options, more details are provided below.

Since PV spectral gains or losses are relative to performance under the reference AM1.5 spectral distribution, the simplest benchmark is simply to assume the AM1.5 spectrum at all times, i.e., to ignore spectral effects altogether and have a fixed spectral mismatch factor of 1 (see Section V.A.).

Another benchmark available at the five Canadian stations is the spectral irradiance over the 280–4000-nm range modeled by Spectrafy using the SolarSIM-G measurements as inputs [14].

Under cloudless conditions, spectral modeling is much easier than under clouds. It is thus possible to use the SMARTS model (version 2.9.9) to derive estimates of the incident irradiance's spectral distribution [15, 16]. For the best results, ground-based observations (such as from AERONET) of the most radiatively-important atmospheric quantities—aerosols and water vapor—must be used as inputs. Here, three sites (Almería, Egbert, and Golden) have a collocated AERONET station, whose information is appropriately used to obtain "SMARTS-Reference" predictions.

Modeled atmospheric data, such as provided by MERRA-2, can also be used with SMARTS, but should be expected to yield spectral irradiance estimates of lower quality because of the significant uncertainty in the MERRA-2 aerosol products, in particular [17]. In this analysis, the MERRA-2 aerosol and water vapor products are used with no correction or interpolation of any kind. Stated differently, this information is exactly that for the whole grid cell containing each experimental site. This is contrary to the situation for the NSRDB broadband and spectral (NSRDB-S) products, for which the MERRA-2 information is subjected to various preliminary corrections [18].

In spite of this, the use of SMARTS (with inputs from uncorrected MERRA-2 information in particular) constitutes a particularly relevant benchmark for NSRDB-S because the FARMS-NIT model is intended to mimic SMARTS under clear-sky conditions.

V. Model Evaluation

Spectral irradiances for a horizontal plane are extracted for the North American sites using the NSRDB Data Viewer. For Almería, the CM-SAF SRI data on a horizontal plane are normally provided on a daily or monthly resolution through the CM-SAF portal. In the present case, 30-minute data from June 1, 2018 to June 30, 2019 have been obtained via personal communication.

As detailed below, the NSRDB-S and CM-SAF SRI products are first evaluated over all time steps ("all-sky") in terms of

their skill at modeling PV spectral effects. The analysis is then restricted to clear-sky conditions and extended to include direct comparisons of spectral distributions to help diagnose differences between the satellite products and both the WISER and SolarSIM-G all-sky benchmarks.

A. All-sky analysis and PV spectral effect comparisons

Instantaneous PV spectral effects can be encapsulated via the spectral mismatch factor (SMM), defined as [19]:

$$SMM = \frac{\int_a^b s(\lambda)E_{meas}(\lambda)d\lambda}{\int_a^b s(\lambda)E_{ref}(\lambda)d\lambda} \frac{\int_c^d s_{ref}(\lambda)E_{ref}(\lambda)d\lambda}{\int_c^d s_{ref}(\lambda)E_{meas}(\lambda)d\lambda} \quad (1)$$

where $s(\lambda)$ is the spectral responsivity of the PV module of interest, $s_{ref}(\lambda)$ is the spectral responsivity of the device used to measure broadband irradiance, $E_{meas}(\lambda)$ is the measured spectral irradiance, $E_{ref}(\lambda)$ is a reference spectral irradiance (i.e., the AM1.5 standard global spectrum) and a, b, c and d are the endpoints of the ranges over which $s(\lambda)$ and $s_{ref}(\lambda)$, respectively, are non-zero.

Spectral effects can be incorporated into PV modeling by replacing the broadband measured irradiance E_{meas} by the effective irradiance E_{eff} with:

$$E_{eff} = SMM \times E_{meas} \quad (2)$$

For the purposes of this study, the long-term spectral derate factor (SDF) applicable to PV energy yield is defined independently of PV modeling as:

$$\text{SDF} = \frac{\sum SMM \times E_{meas}}{\sum E_{meas}} \quad (3)$$

where the sums include all data in the period of interest.

SMM is computed here for each site at each available time step and for six PV module technologies: amorphous silicon (a-Si), copper indium gallium selenide (CIGS), monocrystalline silicon (mono-Si), polycrystalline silicon (poly-Si), and two cadmium telluride technologies from First Solar, namely series 4-1 and earlier (FS4-1), and series 4-2 and later (FS4-2). The spectral responsivities for each PV module type [3] are shown in Fig. 2.

At each site, calculations of SMM and SDF are performed for all measured, satellite-based, and benchmark model data, after necessary filtering to retain only common time steps, and with SMM computed over common wavebands: 280–4000 nm at the Canadian sites, 290–1650 nm at Golden, and 307–1613 nm at Almería. Performance is assessed for each site and PV module technology via the mean absolute deviation (MAD) in SMM and the deviation in SDF relative to a chosen reference. For Golden and Almería, the WISER measurements act as the reference, whereas the SolarSIM-G modeled spectra are selected as the reference for the Canadian sites under all-sky conditions.

B. Clear-sky analysis and spectra comparisons

The clear-sky analysis is conducted for the three stations with AERONET data, i.e., Egbert, Almería, and Golden. Clear-sky periods are identified first by running the Bright-Sun [20] algorithm with measurements of the three irradiance components, as well as clear-sky irradiance estimates from the Copernicus Atmosphere Monitoring Service (CAMS) McClear model [21] as inputs. To ensure clear-sky conditions for satellite products as well, the analysis is further restricted to instants when the NSRDB-S clear-sky and all-sky GHI values are equal, or within 4% of each other for CM-SAF SRI.

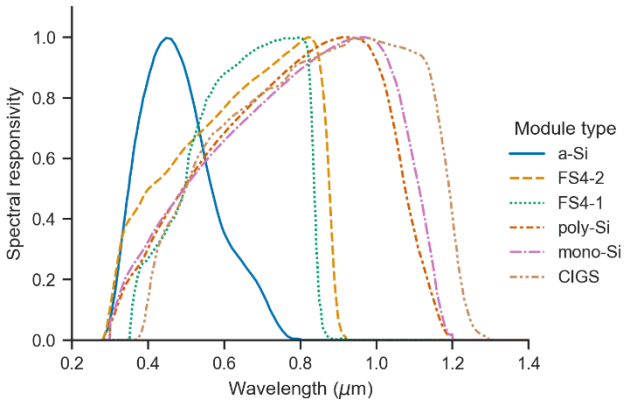

Fig. 2. Normalized spectral responsivities of six PV module technologies.

In addition to the analysis of PV spectral effects, the satellite-based spectra are directly compared to the different benchmark spectra under clear skies. At Golden, the measured WISER data have a limited optical resolution, leading to smoother spectra than in modeled benchmarks. The NSRDB-S and SMARTS spectra are therefore smoothed using a Gaussian moving average [15] based on a full width at half maximum of 6.5 nm for the MS-711 and MS-712 instruments, and 4.5 nm for the MS-710. In contrast, for Almería, the CM-SAF SRI product provides irradiance in only 32 spectral bands, thus all other spectra are arranged in the same way to make waveband-by-waveband comparisons possible. Similarly, all spectra are normalized to a broadband irradiance of 1000 W/m^2 over the common wavebands detailed in Section V.A. Mean normalized spectra are compared, and mean percent deviations computed, with the WISER instruments acting as references at Almería and Golden, and the SMARTS-Reference model at Egbert.

VI. Results and Discussion

A. All-sky

For CM-SAF SRI at Almería, the SMM's MAD and the deviation in SDF are shown for each PV module technology in Figs. 3 and 4, respectively, alongside the corresponding metrics when spectral effects are ignored ("No spectral" benchmark). Figs. 5 and 6 show the same metrics for NSRDB-S, with the minimum, mean, and maximum deviations across the six North American sites. Note that these deviations must be interpreted with care, since in many cases they are comparable to the uncertainties in SMM (and SDF) themselves: according to an analysis for one site in Germany [22], standard uncertainties on SMM for an EKO WISER are ≈0.009 for crystalline silicon and ≈0.018 for a-Si.

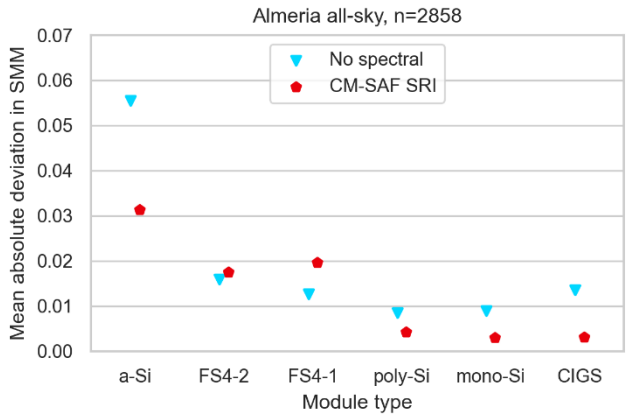

Fig. 3. Mean absolute deviation in all-sky SMM related to WISER at Almería for CM-SAF SRI and the "No spectral" benchmark, for each PV module technology.

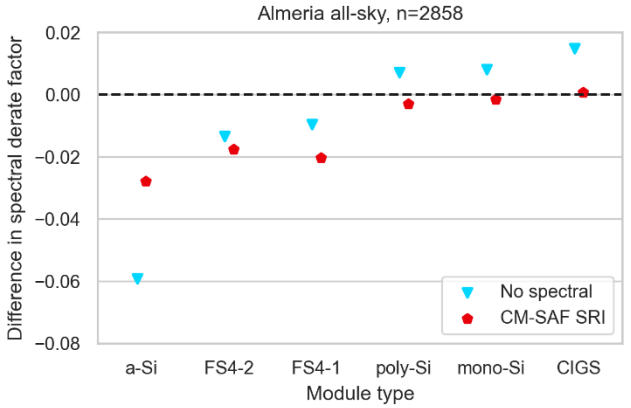

Fig. 4. Difference in all-sky SDF at Almería relative to the WISER for CM-SAF SRI and the "No spectral" benchmark, for each PV module technology.

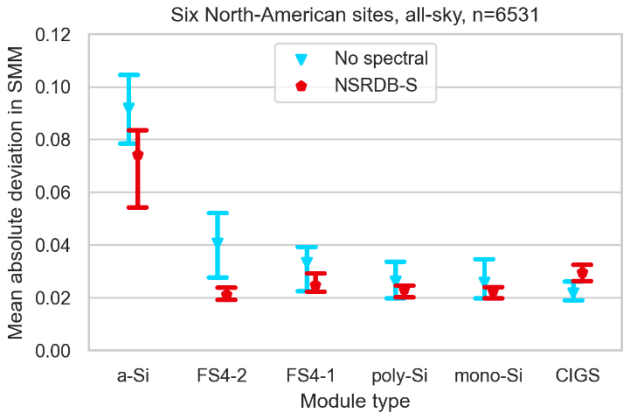

Fig. 5. Mean absolute deviation in all-sky SMM for the NSRDB-S and the "No spectral" benchmark for each module type, relative to the WISER or SolarSIM-G values, depending on site. Bars denote maxima and minima across the six North American sites and the marker denotes the mean.

With this caveat in mind, the results of the all-sky analysis nevertheless provide some indications about the NSRDB-S and CM-SAF SRI skills relative to the "No spectral" benchmark. For SRI, results suggest that it outperforms the simple benchmark at Almería in terms of estimating SMM and SDF, except for the cadmium telluride modules. The difference is most significant for a-Si, whose spectral effects are largest.

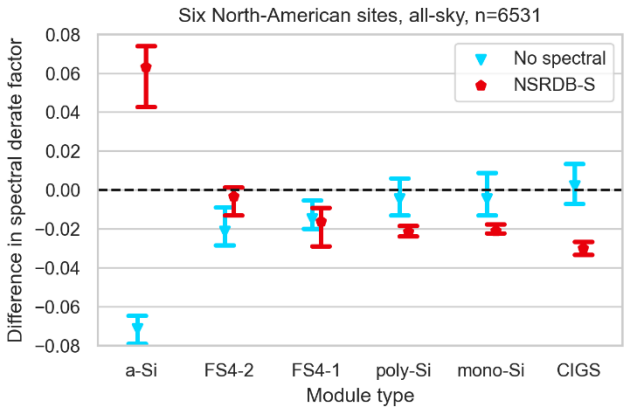

Fig. 6. Differences in all-sky SDF for the NSRDB-S and the "No spectral" benchmark for each module type, relative to the WISER or SolarSIM-G values, depending on site. Bars denote maxima and minima across the six North American sites and the marker denotes the mean.

In the case of NSRDB-S, the mean absolute deviations tend to be smaller than for the "No spectral" benchmark relative to the WISER and SolarSIM-G values, but the reverse is true when considering SDF. Moreover, the deviations in the latter are fairly consistent across the six locations, suggesting that there may be systematic errors in the NSRDB-S spectra. This hypothesis is explored for clear-sky conditions in the next section.

B. Clear-sky

Fig. 7 displays box plots of the clear-sky SMM distribution for each PV technology at Golden to emphasize differences in temporal variance. The plot is for 54 clear-sky periods during a few months of 2014, when a temporary AERONET station operated at Golden. Contrary to Fig. 5, NSRDB-S glaringly underperforms compared to all other spectral determinations, and even to the "No spectral" benchmark (SMM=1), both in terms of mean value and distribution properties. At the other extreme, the two SMARTS-based results behave very similarly and outperform that benchmark, except for the FS4-1 and FS4-2 modules. Fig. 7 also underlines the particular case constituted by a-Si modules, whose clear-sky SMM is much higher than that of any other module technology. Interestingly, this clear-sky a-Si SMM is smaller at Almería (Fig. 8). Although CM-SAF SRI's mean SMM is different from that of the other determinations, its dispersion around the mean is similar. This is not the case with NSRDB-S at Golden (Fig. 7).

Fig. 9 provides a comparison of the mean clear-sky spectra obtained at Golden in 2014 from the WISER measurements and the predictions of NSRDB-S and SMARTS (using two alternate sets of inputs), all obtained after the normalization process described in Section V.B. The two SMARTS-based mean spectra agree with the WISER's mean spectrum to within about ±3%, except around strong atmospheric absorption bands (a typical issue; see [16]) and in the UV.

In contrast, the NSRDB-S mean spectrum displays a very different behavior. The shape of the difference curve (bottom of Fig. 9), with overestimation below 500 nm and underestimation beyond, was not expected. This is also seen at Egbert, and is

likely related to a too-low aerosol optical depth and/or an incorrect modeling of the aerosol transmittance, but the exact cause of this issue will require further scrutiny. Considering the spectral responsivity curves from Fig. 2 for the six PV module technologies, this pattern is consistent with the systematic overestimation of SDF by NSRDB-S for a-Si across all North-American sites seen in Fig. 6, and the underestimation for other PV technologies.

Finally, Fig. 10 is similar to Fig. 9, but for the conditions of Almería. The spectral resolution of the mean CM-SAF SRI spectrum is obviously very limited compared to that of NSRDB-S, and some of its 32 wavebands appear to be somewhat biased, even though comparatively less than the latter below 500 nm. A tentative explanation for these biases is that SRI is modeled using a monthly aerosol climatology and monthly-mean water vapor data, rather than dynamic hourly information, as with MERRA-2. These localized biases in the SRI spectra can explain why the clear-sky SRI's a-Si SMM box plot is not exactly aligned with those of the modeled spectra, as displayed in Fig. 8.

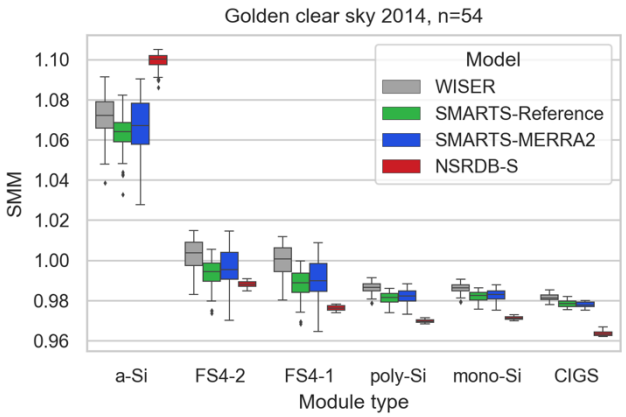

Fig. 7. Box-plot distributions of clear-sky SMM at Golden during 2014 for each module type, as obtained from the WISER, NSRDB-S, and SMARTS predictions with two sets of inputs.

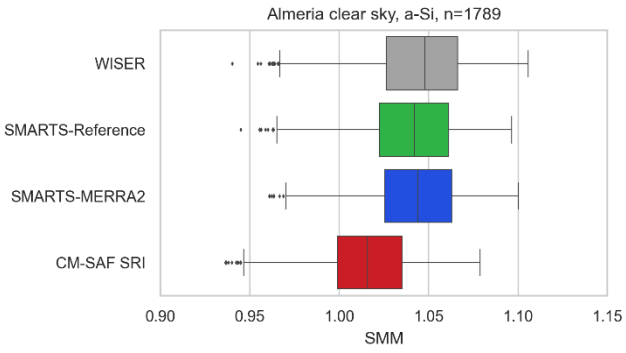

Fig. 8. Box-plot distributions of clear-sky SMM at Almería during 2018–2019 for an a-Si module, as obtained from the WISER, CM-SAF SRI, and SMARTS predictions with two sets of inputs.

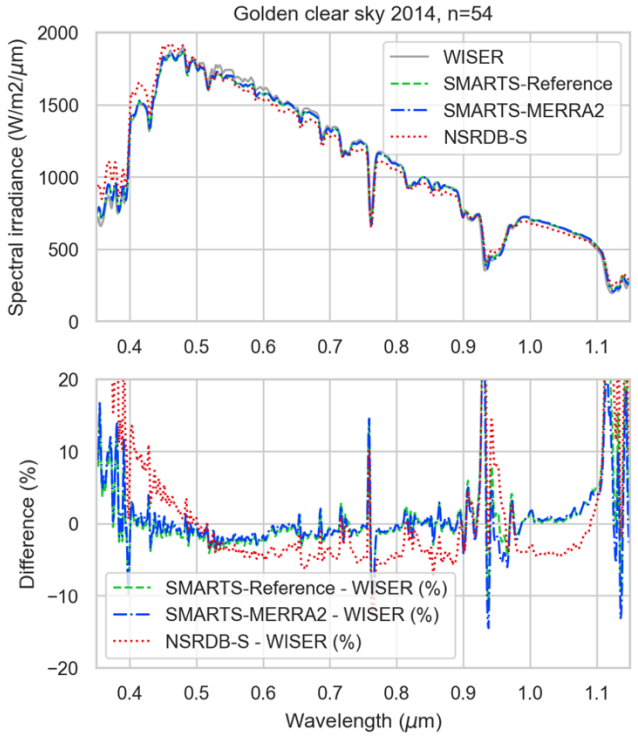

Fig. 9. Mean normalized clear-sky spectra at Golden in 2014 from WISER, NSRDB-S, and SMARTS (with two sets of inputs), after smoothing of the modeled spectra at the WISER resolution (top); spectral differences between these mean modeled spectra and the mean WISER observations (bottom).

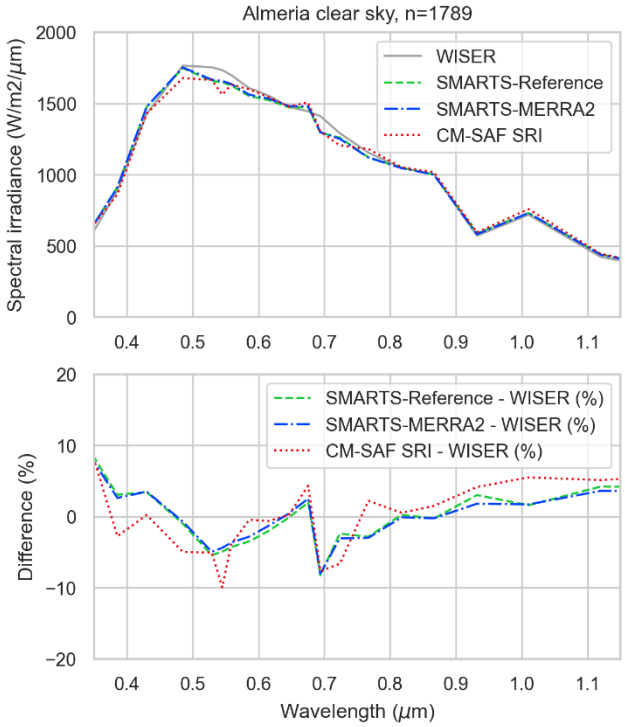

Fig. 10. Mean normalized clear-sky spectra at Almería from WISER, CM-SAF SRI, and SMARTS (with two sets of inputs), after summing the modeled spectra over CM-SAF SRI wavebands (top); spectral differences between these mean modeled spectra and the mean WISER observations (bottom).

VII. Conclusion

Satellite-based spectral irradiance products offer a promising avenue for estimating PV spectral effects over broad geographic areas. The analysis of CM-SAF SRI at Almería indicates that this product generally has skill with respect to a simple benchmark of excluding spectral effects. In contrast, results for the NSRDB Spectral On-Demand (NSRDB-S) service at six sites in North America reveal systematic differences between the NSRDB-S and both the SolarSIM-G and WISER estimates. Comparisons of spectra under clear-sky conditions suggest these discrepancies might be due in part to the treatment of aerosols in NSRDB-S. Furthermore, the SMARTS-Reference and SMARTS-MERRA2 mean spectra are in good agreement at those three sites having a collocated AERONET station. This finding holds promise for clear-sky spectral modeling if it generalizes to other sites because MERRA-2 has worldwide coverage and provides gapless hourly data streams starting in 1980.

Acknowledgment

We thank Viktar Tatsiankou from Spectrafy, Stefan Wilbert from DLR, Afshin Andreas from NREL, and Uwe Pfeifroth and Jörg Trentmann from DWD for help with acquiring spectral irradiance data. The Principal Investigators and personnel of the three AERONET stations used in this work were also instrumental to the success of the study.

References

[1] *Photovoltaic devices – Part 3: Measurement principles for terrestrial photovoltaic (PV) solar devices with reference spectral irradiance data*, IEC 60904-3:2019, Feb. 15, 2019.

[2] J. Polo, M. Alonso-Abella, J. A. Ruiz-Arias, and J. L. Balenzategui, "Worldwide analysis of spectral factors for seven photovoltaic technologies," *Solar Energy*, vol. 142, pp. 194–203, 2017.

[3] S. Pelland, C. Beswick, D. Thevenard, A. Côté, A. Pai, and Y. Poissant, "Development and testing of the PVSPEC model of photovoltaic spectral mismatch factor," in *Proc. 47th IEEE Photovoltaic Specialists Conference (PVSC)*, pp. 1258–1264, 2020.

[4] R. Müller, U. Pfeifroth, C. Träger-Chatterjee, J. Trentmann, and R. Cremer, "Digging the METEOSAT treasure—3 decades of solar surface radiation," *Remote Sensing*, vol. 7, pp. 8067–8101, 2015.

[5] Y. Xie and M. Sengupta, "A Fast All-sky Radiation Model for Solar applications with Narrowband Irradiances on Tilted surfaces (FARMS-NIT)," *Solar Energy*, vol. 174, pp. 691-702, 2018.

[6] Y. Xie, M. Sengupta, and C. Wang, "A Fast All-sky Radiation Model for Solar applications with Narrowband Irradiances on Tilted surfaces (FARMS-NIT): Part II. The cloudy-sky model," *Solar Energy*, vol. 188, pp. 799–812, 2019, doi: 10.1016/j.solener.2019.06.058.

[7] R. Gelaro et al., "The Modern-Era Retrospective Analysis for Research and Applications, Version 2 (MERRA-2)," *Journal of Climate*, vol. 30, no. 14, July 2017, doi: 10.1175/JCLI-D-16-0758.1.

[8] C. A. Gueymard, "Prediction and validation of cloudless shortwave solar spectra incident on horizontal, tilted, or tracking surfaces," *Solar Energy*, vol. 82, pp. 260–271, 2008, doi:10.1016/j.solener.2007.04.007.

[9] U. Pfeifroth, S. Kothe, R. Müller, J. Trentmann, R. Hollmann, P. Fuchs, and M. Werscheck, "Surface Radiation Data Set - Heliosat (SARAH) - Edition 2", Satellite Application Facility on Climate Monitoring, doi: 10.5676/EUM_SAF_CM/SARAH/V002.

[10] R. Mueller, T. Behrendt, A. Hammer, and A. Kemper, "A new algorithm for the satellite-based retrieval of solar surface irradiance in spectral bands," *Remote Sensing*, vol. 4, pp. 622–647, 2012.

[11] C. Anderson, "Benchmarking of different solar spectra quality control methods", M.S. thesis, Queensland University of Technology, Brisbane, QLD, Australia, 2020.

[12] B. N. Holben, T. F. Eck, I. Slutsker, D. Tanré, J. P. Buis, A. Setzer, E. Vermote, J. A. Reagan, Y. J. Kaufman, T. Nakajima, F. Lavenu, I. Jankowiak, A. Smirnov, "AERONET—a federated instrument network and data archive for aerosol characterization," *Remote Sens. Environ.* vol. 66, pp. 1–16, 1998.

[13] D. M. Giles, A. Sinyuk, M. G. Sorokin, J. S. Schafer, A. Smirnov, I. Slutsker, T. F. Eck, B. N. Holben, J. R. Lewis, J. R. Campbell, E. J. Welton, S. V. Korkin, A. I. Lyapustin, "Advancements in the Aerosol Robotic Network (AERONET) Version 3 database – automated near-real-time quality control algorithm with improved cloud screening for Sun photometer aerosol optical depth (AOD) measurements," *Atmos. Meas. Tech.* vol. 12, pp. 169–209, 2019.

[14] V. Tatsiankou, K. Hinzer, H. Schriemer, P. McVey-White, and R. Beal "Efficient, real-time global spectral and broadband irradiance acquisition", in *2018 IEEE 7th World Conference on Photovoltaic Energy Conversion*, pp. 2362 - 2365, 2018, doi: 10.1109/PVSC.2018.8547671.

[15] C. A. Gueymard, "Parameterized transmittance model for direct beam and circumsolar spectral irradiance," *Solar Energy*, vol. 71, pp. 325-346, 2001, doi: 10.1016/S0038-092X(01)00054-8.

[16] C. A. Gueymard, "The SMARTS spectral irradiance model after 25 years: New developments and validation of reference spectra," *Solar Energy*, vol. 187, pp. 233-253, 2019, doi: 10.1016/j.solener.2019.05.048; Corrigendum, doi:10.1016/j.solener.2022.02.046.

[17] C. A. Gueymard and D. Yang, "Worldwide validation of CAMS and MERRA-2 reanalysis aerosol optical depth products using 15 years of AERONET observations," *Atmos. Environ.*, vol. 225, 117216, 2020.

[18] M. Sengupta, Y. Xie, A. Habte, G. Buster, G. Maclaurin, P. Edwards, H. Sky, M. Bannister, and E. Rosenlieb, "The National Solar Radiation Database (NSRDB) Final Report: Fiscal Years 2019–2021," National Renewable Energy Laboratory Tech. Rep. NREL/TP-5D00-82063, 2022.

[19] *Photovoltaic devices - Part 7: Computation of the spectral mismatch correction for measurements of photovoltaic devices*, IEC 60904-7 ED4, August 20, 2019.

[20] J. M. Bright, X. Sun, C. A. Gueymard, B. Acord, P. Wang, N. A. Engerer, "Bright-Sun: A globally applicable 1-min irradiance clear-sky detection model," *Renewable and Sustainable Energy Reviews*, vol. 121, 109706, 2020, doi: 10.1016/j.rser.2020.109706.

[21] B. Gschwind, L. Wald, P. Blanc, M. Lefèvre, M. Schroedter-Homscheidt, and A. Arola, "Improving the McClear model estimating the downwelling solar radiation at ground level in cloud-free conditions ─ McClear-v3", *Meteorologische Zeitschrift*, vol. 28, pp. 147-163, 2019.

[22] D. Dirnberger, B. Müller, and C. Reise, "On the uncertainty of energetic impact on the yield of different PV technologies due to varying spectral irradiance," *Solar Energy*, vol. 111, pp. 82-96, 2015.